Molecular Biology of the Cell
Vol. 12, 2614–2628, September 2001

# Aux1p/Swa2p Is Required for Cortical Endoplasmic Reticulum Inheritance in *Saccharomyces cerevisiae*

**Yunrui Du,*† Marc Pypaert,* Peter Novick,* and Susan Ferro-Novick*†‡**

*Department of Cell Biology and †Howard Hughes Medical Institute, Yale University, New Haven, Connecticut 06519-1418

Submitted December 21, 2000; Revised May 4, 2001; Accepted June 17, 2001
Monitoring Editor: David Drubin

In the yeast *Saccharomyces cerevisiae*, the endoplasmic reticulum (ER) is found at the periphery of the cell and around the nucleus. The segregation of ER through the mother-bud neck may occur by more than one mechanism because perinuclear, but not peripheral ER, requires microtubules for this event. To identify genes whose products are required for cortical ER inheritance, we have used a Tn3-based transposon library to mutagenize cells expressing a green fluorescent protein-tagged ER marker protein (Hmg1p). This approach has revealed that *AUX1/SWA2* plays a role in ER inheritance. The COOH terminus of Aux1p/Swa2p contains a J-domain that is highly related to the J-domain of auxilin, which stimulates the uncoating of clathrin-coated vesicles. Deletion of the J-domain of Aux1p/Swa2p leads to vacuole fragmentation and membrane accumulation but does not affect the migration of peripheral ER into daughter cells. These findings suggest that Aux1p/Swa2p may be a bifunctional protein with roles in membrane traffic and cortical ER inheritance. In support of this hypothesis, we find that Aux1p/Swa2p localizes to ER membranes.

## INTRODUCTION

The endoplasmic reticulum (ER) is an essential organelle required for protein assembly, lipid biosynthesis, and vesicular traffic in eukaryotic cells (Nunnari and Walter, 1996). The ER generally consists of an elaborate network of interconnected membrane tubules that connects to the nuclear envelope (Palade, 1956; Prinz *et al.*, 2000). The spatial arrangement of cytoplasmic ER can vary in different cell types. In animal cells, the ER consists of a meshwork that is physically contiguous with the nuclear envelope and emanates throughout the cytoplasm (Palade, 1956). In the budding yeast *Saccharomyces cerevisae,* the ER consists of a cortical network that is closely apposed to the plasma membrane (cortical ER) with tubular connections to the nuclear envelope (perinuclear ER) (Preuss *et al.*, 1991). Although the outer membrane of the nuclear envelope appears to be biochemically and functionally similar to the ER, some proteins, such as binding proteins for the nuclear lamina, are restricted to the inner membrane of the nuclear envelope (Wilson, 2000). In addition, the ER itself can be divided into several subdomains with specific structures and functions, including transitional, rough, and smooth ER. The transitional ER is the region where carrier vesicles are formed. These vesicles serve to transport cargo to the Golgi apparatus. In higher eukaryotic cells, the rough ER is studded with ribosomes carrying nascent polypeptide chains that are in the process of translocating into the lumen, whereas the smooth portions are free of bound ribosomes. Both the cortical ER and the nuclear envelope in yeast have been shown to contain associated ribosomes (Baba and Osumi, 1987). However, because of the abundance of free ribosomes in the yeast cytoplasm, it is difficult to determine whether there are also smooth portions of ER in yeast cells. In addition, a close association of mitochondria with subdomains of the ER has been described. Despite its complex structure, the ER is dynamic, undergoing continuous formation of new tubules and movement of individual tubules (Lee and Chen, 1988; Prinz *et al.*, 2000). The molecular mechanisms that establish the morphology, distribution, and dynamics of the ER remain poorly understood.

A prominent feature of the cell cycle is the accurate segregation of the ER and other membrane-bounded organelles into daughter cells. In *Saccharomyces cerevisae*, both the cortical ER and nuclear envelope remain intact during mitosis. Electron microscopic studies have shown that ER tubules are transported into the growing bud after secretory vesicles appear, but before the segregation of vacuoles and mitochondria (Preuss *et al.*, 1991; Preuss *et al.*, 1992). The nuclear envelope enters the bud even later as a consequence of nuclear division. The nucleus first migrates to the mother-bud neck then undergoes extension into the bud and division. Each of these nuclear processes requires microtubules (Huffaker *et al.*, 1988; Jacobs *et al.*, 1988).

In mammalian cells, it has been thought that the nuclear envelope undergoes fragmentation into vesicles in late prophase. The vesicles are then dispersed throughout the cytoplasm and are ultimately reassembled into two nuclei

‡ Corresponding author. E-mail address: susan.ferronovick@yale.edu.

**Table 1.** Yeast strains used in this study

| Strain | Genotype | Source |
|---|---|---|
| NY873 | *MAT***a** *his3-Δ200 leu2-3,112 lys2-801 ura3-52* | Novick lab collection |
| NY870 | *MATα his3-Δ200 leu2-3,112 lys2-801 ura3-52* | Novick lab collection |
| NY1211 | *Matα Gal*$^+$ *his3-Δ200 leu2-3,112 ura3-52* | Novick lab collection |
| SFNY26-3A | *MAT***a** *ura3-52* | Ferro-Novick lab collection |
| SFNY1054 | *MAT***a** *his3-Δ200 leu2-3,112 lys2-801 ura3-52::(URA3 hmg1-GFP)* | This study |
| SFNY1060 | *MATα his3-Δ200 leu2-3,112 lys2-801 ura3-52::(URA3 hmg1-GFP)* | This study |
| SFNY1061 | *MAT***a**/*α his3-Δ200/his3-Δ200 leu2-3,112/leu2-3,112 lys2-801/lys2-801 ura3-52::(URA3 hmg1-GFP)/ura3-52::(URA3 hmg1-GFP)* | This study |
| SFNY1053 | *MAT***a** *his3-Δ200 leu2-3,112 lys2-801 ura3-52::(URA3 hmg1-GFP) aux1/swa2:(aux1/swa2::Tn3 LEU2)* | This study |
| SFNY1055 | *MAT***a** *his3-Δ200 leu2-3,112 lys2-801 ura3-52::(URA3 hmg1-GFP) aux1/swa2::his5*$^+$ | This study |
| SFNY1094 | *MAT***a** *his3-Δ200 leu2-3,112 lys2-801 ura3-52 AUX1/SWA2::(AUX1/SWA2-GFP, his5*$^+$*)* | This study |
| GPY982 | *MATα chc1-521 leu2-3,112 his3Δ200 trp1-Δ901 lys2-801 suc2-Δ9 GAL* | Payne lab collection |
| SFNY1089 | *MATα chc1-521 leu2-3,112 his3Δ200 trp1-Δ901 lys2-801 suc2-Δ9 GAL ura3-52::(URA3 hmg1-GFP)* | This study |
| DBY5404 | *MAT***a** *his3-Δ200 leu2-3,112 trp1-1 ura3-52 arf1::HIS3* | Botstein lab collection |
| SFNY1090 | *MAT***a** *his3-Δ200 leu2-3,112 trp1-1 arf1::HIS3 ura3-52::(URA3 hmg1-GFP)* | This study |

by homotypic fusion during telophase (Wiese and Wilson, 1993; Marshall and Wilson, 1997). However, a new model has been suggested based on the recent observation that inner nuclear membrane proteins become dispersed throughout the ER during mitosis. By this model, the nuclear envelope is absorbed into cytoplasmic ER and consequently the partitioning of components of the nuclear envelope is mediated by the segregation of cytoplasmic ER (Ellenberg *et al.*, 1997; Yang *et al.*, 1997). Although vesicularization of the cytoplasmic ER network during mitosis has been reported in several cell types, the cytoplasmic ER network in most higher eukaryotic cells retains its reticular morphology during mitosis, just as in yeast (Zeligs and Wollman, 1979; Waterman-Storer *et al.*, 1993; Ioshii *et al.*, 1995; Ellenberg *et al.*, 1997; Terasaki, 2000). Given its low copy number, the intact ER network is unlikely to be accurately partitioned simply by random diffusion throughout the mitotic cell (Warren and Wickner, 1996). The mechanisms controlling the inheritance of the ER network are as yet undetermined. Furthermore, little is known about the coordination of ER inheritance with other processes during cell proliferation.

*Saccharomyces cerevisae* grow in a highly polarized manner in which virtually all growth occurs in the bud. This feature, in combination with the ease by which this organism can be genetically manipulated, has helped to reveal many insights into the molecular details of organelle inheritance. The isolation of yeast mutants defective in the segregation of mitochondria and vacuoles has led to the identification of proteins involved in these events (McConnell *et al.*, 1990; Weisman *et al.*, 1990; Yaffe, 1999). We have initiated a screen to identify mutants that exhibit defects in the segregation of cortical ER during mitosis. Here we describe the analysis of one of the genes identified and the properties of the gene product.

## MATERIALS AND METHODS

### *Plasmid and Strain Construction*

Plasmid pYDY104 (*CEN*, *LEU2*) encodes a mitochondria-targeting sequence that is fused to the $NH_2$ terminus of the red fluorescent protein (RFP) and whose expression is driven by the constitutive *GPD* promoter. To construct this plasmid, a 0.9-kb *Xba*I/*Xho*I fragment from p416-*GAL1*+PrFoATP-dsREDFP (Mozdy *et al.*, 2000) was cloned into p415-*GPD* (Mumberg *et al.*, 1995) between the *Xba*I and *Xho*I sites.

SFNY1054, SFNY1060, SFNY1089, and SFNY1090 (Table 1) were constructed by transforming NY873, NY870, GPY982, and DBY5404, respectively, with pRH475 after it was digested with *Stu*I (Cronin *et al.*, 2000) and selecting for Ura$^+$ transformants.

Aux1p/Swa2p-GFP (SFNY1094) was constructed by tagging the 3′ end of *AUX1/SWA2* in NY873 with green fluorescent protein (GFP)-encoding sequences with the use of a polymerase chain reaction (PCR)-mediated gene modification method developed by Longtine *et al.* (1998). The 5′ end of the forward primer (p1204CTAG: 5′-GTACTTTAAGTATTGCTTGGGATAAGTTCAAACTGCAGAATGACATTAACCGGATCCCCGGGTTAATTAA-3′) and the reverse primer (p1204CD2: 5′-AAAGTACATATCAAAAACAACTGAGC-GAAGCAGGCACACAAGGGAAATCAGAATTCGAGCTCGTTTAAAC-3′) contained 50 nucleotides corresponding to *AUX1/SWA2* gene-specific sequences just upstream and downstream of the stop codon, respectively. The GFP(S65T)-expressing sequences on plasmid pFA6a-GFP(S65T)-His3MX6 (Longtine *et al.*, 1998) were amplified with the use of p1204CTAG and p1204CD2, transformed into NY873, and the His$^+$ transformants were selected.

### *Isolation of Mutants*

Insertional mutagenesis of the yeast genome was performed with the use of a library of yeast genomic fragments containing random insertions of a mini-Tn3::*lacZ*::*LEU2* transposon (Burns *et al.*, 1994). The mutagenized DNA fragments were digested with *Not*I and transformed into SFNY1054 or SFNY1060. The Leu$^+$ transformants were grown at 30°C in 100 μl of selective medium lacking leucine in Microtest 96-well tissue culture plates (Becton Dickinson, San Jose,

CA) to log phase and examined in a Zeiss Axiophot fluorescence microscope. Mutants of interest were recultured in 100 μl of selective medium in 96-well plates and in 5 ml of selective medium with good aeration. Those strains that reproducibly exhibited significant defects in cortical ER inheritance were purified and saved for further characterization.

## *Cloning and Disruption of AUX1/SWA2*

The location of the transposon in the *aux1/swa2::Tn3* mutant was identified by a PCR-mediated method (Adams *et al.*, 1997) with minor modifications as follows. Briefly, to achieve intramolecular circularization of genomic DNA, 2.5 μg of DNA was digested with *Rsa*I and ligated with 400 U of T4 DNA ligase in a 250-μl reaction. A pair of inverse PCR primers (INPCR1: 5′-TAAGTTGGGTAACGCCAGGGTTTTC-3′ and INPCR2: 5′-TTCCATGTTGCCACTCGCTTTAATG-3′) corresponding to the ends of a 738-bp *Rsa*I-digested fragment at the 5′ end of the transposon were used to amplify genomic sequences adjacent to the transposon. A single band of ~350-bp, which was not observed in the wild-type control, was purified from an agarose gel and sequenced with the use of the INPCR1 primer. The insertion site was then determined by comparing the genomic sequences with those in the *S. cerevisiae* Genome Database with the use of the BLAST program.

SFNY1055 (*aux1/swa2*Δ) was constructed by a PCR-mediated gene deletion method developed by Longtine *et al.* (1998). The 5′ end of the forward primer (p1204CD5: 5′-ATTCCTGTGCTTCTGGAAAGGACGCAGCCTGCAAGAAACAGTCAACATCATG ACGGATCCCCGGGTTAATTAA-3′) and the reverse primer (p1204CD2: 5′-AAAGTACATATCAAAAACAACTGAGCGAAGCAGGCACACAAGGGAAATCAGAATTCGAGCTCGTTTAAAC-3′) contained 50 nucleotides corresponding to *AUX1/SWA2* gene-specific sequences just upstream of the start codon and just downstream of the stop codon, respectively. The *Schizosaccharomyces pombe his5*$^+$ gene on the plasmid pFA6a-His3MX6 (Longtine *et al.*, 1998) was amplified with the use of p1204CD5 and p1204CD2, transformed into SFNY1054, and His$^+$ transformants were selected. Replacement of the *AUX1/SWA2* ORF with the *his5*$^+$ gene was confirmed by PCR with the use of primers p3679A (5′-AACAAGTGCAGGCTAACATACTTTC-3′) and p1204CD4 (5′-CAAATTGGGTGCC ACTTGTAAGTCA-3′) that correspond to the 5′ and 3′ untranslated region of *AUX1/SWA2*, respectively. By the same method SFNY1070 (*aux1/swa2*Δ*c*) was constructed. Codons corresponding to the last 161 amino acid (508–668) of Aux1p/Swa2p in SFNY1070 were deleted with the use of the primer pair p1204CD1 (5′-AAGAGCTGATTAAGAAGAATTTTTTTGATGATAAAATCATGCAGGGAAAATGACGGATCCCCG GGTTAATTAA-3′) and p1204CD2. The truncation was confirmed by PCR with the use of primers p1204CD3 (5′-CCAAAGATTATGATTAGGCGTGCTG-3′) and p1204CD4. The complete disruption and the COOH-terminal truncation of *AUX1/SWA2* were verified by Western blot analysis with the use of anti-Aux1p/Swa2p polyclonal antibodies increased against an MBP-Aux1p/Swa2p fusion protein.

## *Immunofluorescence Microscopy*

Cells were viewed with a Zeiss Axiophot fluorescence microscope with the use of a Zeiss 100× Plan-Apochromat oil immersion objective. GFP, RFP/C3/FM4–64, and 4′,6-diamidino-2-phenylindole (DAPI) fluorescence were visualized with the use of 480-, 540-, and 365-nm filters, respectively. Images were acquired with the use of the Quantix cooled charge-coupled device camera (Photometrics, Tucson, AZ) controlled by the imaging software IPLab (Scanalytis) and processed with Adobe Photoshop and Adobe Illustrator software.

To visualize ER or mitochondria, cells expressing GFP- or RFP-fusion proteins were grown to log phase ($OD_{600}$ between 0.4 and 0.8) and mounted in growth medium containing 0.3% low melting temperature agarose. Indirect immunofluorescence was performed as follows. A total of five $OD_{600}$ units of log phase cells grown in YPD or selective medium was fixed with an equal volume of 2× fixative solution (2% glucose, 40 mM EGTA, 7.4% formaldehyde) at 25°C for 1 h with gentle shaking. The fixed cells were harvested and washed twice with 5 ml of $NaP_i$/sorbitol buffer (100 mM $NaP_i$, pH 6.6, 1.2 M sorbitol) by vacuum filtration with the use of a Nalgene filter unit (0.2 μm), and resuspended in 3 ml of $NaP_i$/sorbitol buffer. The cells were centrifuged for 5 min at 2400 × *g* in a tabletop centrifuge and the supernatant was aspirated. The cell wall was digested in 1 ml of $NaP_i$/sorbitol buffer containing 143 mM 2-mercaptoethanol and 100 μg/ml zymolase 100T (Seikagaku America, Rockville, MD) during a 14-min incubation at 30°C. Spheroplasts were washed three times with 5 ml of $NaP_i$/sorbitol buffer and resuspended in 500 μl of $NaP_i$/sorbitol buffer. After attachment to poly-L-lysine–coated eight-well microslides, the cells were permeabilized with 0.5% SDS in phosphate-buffered saline/bovine serum albumin (PBS/BSA) buffer (1× PBS, 10 mg/ml BSA), washed 10 times with PBS/BSA, and blocked for 30 min in PBS/BSA in a dark humidified chamber. Primary antibody (1:10,000 anti-Kar2p antisera, 1:500 anti-Sec61p antisera, and 1:2000 monoclonal anti-hemagglutinin (HA) antibody from Berkeley Antibody, Richmond, CA) was diluted in PBS/BSA and incubated for 1 h at room temperature in a dark humidified chamber. The cells were washed 10 times with PBS/BSA and incubated with secondary antibody (1:500 CY3-conjugated goat-antimouse or goat-antirabbit IgG) in PBS/BSA for 1 h at room temperature in a dark humidified chamber. The slides were washed 10 times with PBS/BSA and mounted with Fluoroemount-G (Southern Biotechnology Associates, Birmingham, AL).

When cells were treated with nocodazole, SFNY1054 and SFNY1055 were cultured in YPD to log phase, pelleted, and then resuspended in fresh YPD containing 15 μg/ml nocodazole (3.3 mg/ml stock in dimethyl sulfoxide; Sigma-Aldrich, St. Louis, MO) or 0.45% of dimethyl sulfoxide as a control. After a 3-h incubation at 25°C, >80% of the nocodazole-treated cells contained a large bud and a single unelongated nucleus in the mother cell. The cells were fixed as described above and nuclei were stained by resuspending the fixed cells in mounting medium containing 25 ng/ml DAPI.

Vacuoles in wild-type and *aux1/swa2* mutant cells were labeled with 80 μM FM 4-64 (Molecular Probes, Eugene, OR) according to the method of Wang *et al.* (1996).

## *Electron Microscopy*

Wild-type and *aux1/swa2* mutant cells expressing Hmg1-GFP were grown in YPD at 25°C to log phase and harvested by vacuum filtration with the use of a Nalgene filter unit (0.2 μm). Cells were then prepared for thin-section electron microscopy essentially as described by Mulholland *et al.* (1994). Briefly, the cells were fixed for 60 min at room temperature in a buffer containing 40 mM potassium phosphate, pH 6.7, 0.8 M sorbitol, 1 mM $MgCl_2$, 1 mM $CaCl_2$, 3% paraformaldehyde, and 0.5% glutaraldehyde. After dehydration and embedding in LR White resin, thin sections were cut, collected onto formvar- and carbon-coated nickel grids, and stained with lead citrate and uranyl acetate.

## *Antibody Production*

Rabbit polyclonal antiserum was increased against a purified MBP-Aux1p/Swa2p fusion protein. This fusion protein was constructed by fusing amino acids 4–668 of Aux1p/Swa2p to the maltose binding protein (MBP). The MBP-Aux1p/Swa2p protein was transformed into DH5α cells and induced according to the protocol described in the pMAL Protein Fusion and Purification System manual from New England Biolabs (Beverly, MA). Because the fusion protein was insoluble it was purified by electroelution. Gels were stained with 0.3 M $CuCl_2$ and the correct band was excised, cut into small pieces, and destained three times with 0.25 M Tris pH 9.0, 0.25 M EDTA. After the sample was equilibrated in SDS-PAGE running buffer the fusion protein was electroeluted in a Bio-Rad electroeluter after the manufacturer's instructions. The protein concentration

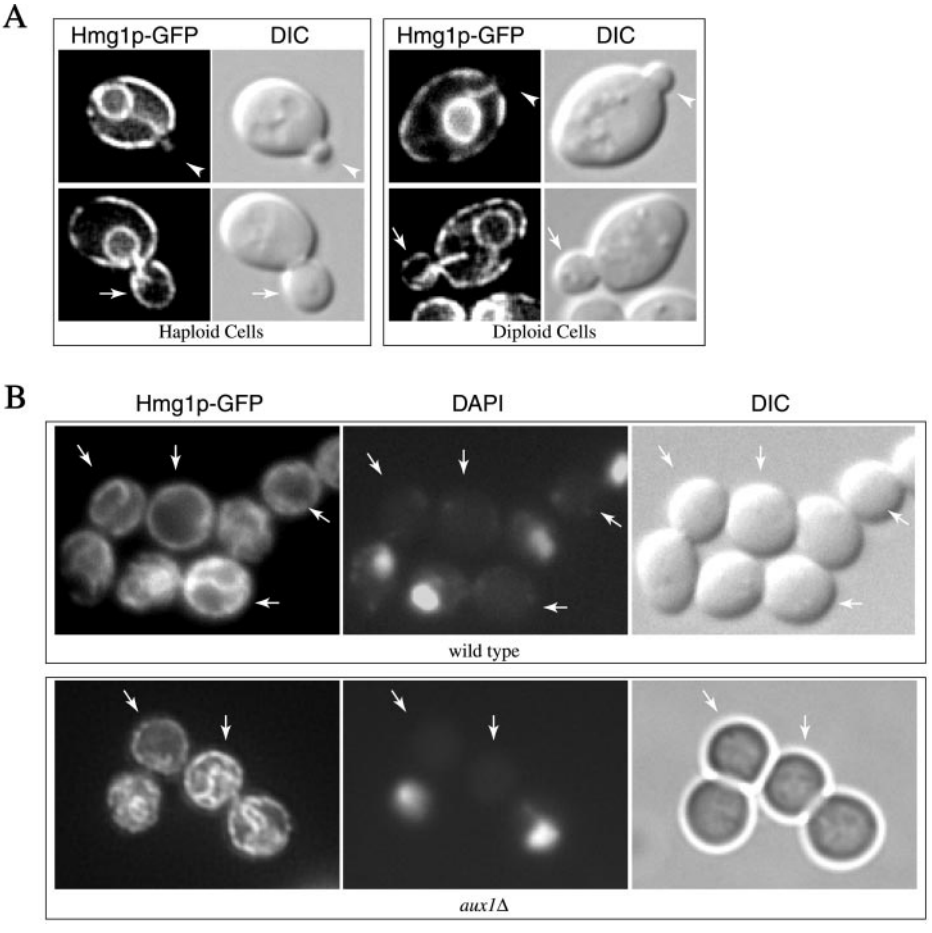


**Figure 1.** (A) Cytoplasmic ER tubules oriented along the mother-bud axis are present through the neck in budded yeast cells. Haploid or diploid wild-type cells expressing Hmg1p-GFP were grown in YPD at 25°C to early log phase and examined by fluorescence microscopy. Arrowheads indicate two representative newly initiated buds that have not acquired detectable cortical ER tubules, whereas arrows point to expanding buds in which the structure of the ER tubules is similar to that in the mother cell. (B) Nocodazole treatment does not significantly affect the inheritance of cortical ER. SFNY1054 (top) and SFNY1055 (bottom) were incubated for 3 h at 25°C in YPD containing 15 $\mu$g/ml nocodazole. After the incubation, cells were fixed and stained with 25 ng/ml DAPI. Arrows point to the enlarged buds of cells blocked in nuclear division.

was determined with a gel assay with the use of BSA as a standard. Antibody to the purified fusion protein was increased in female New Zealand White rabbits with the use of the lymph node protocol.

### *Subcellular Fractionation*

Cells were grown and lysates were prepared exactly as described before (Barrowman *et al.*, 2000). Four hundred $OD_{599}$ units of cells (SFNY26–3A) were fractionated on a sucrose velocity gradient prepared and centrifuged as described before (Barrowman *et al.*, 2000). Fractions (~900 $\mu$l) were collected from the top of the gradient and boiled in SDS sample buffer. Aliquots (90 or 30 $\mu$l) from each fraction were resolved on an SDS-polyacrylamide gel and subjected to immunoblot analysis. Antigens were detected by the enhanced chemiluminescence method (Amersham Pharmacia Biotech, Piscataway, NJ) and the bands were quantified with the use of Bio Image software. The data plotted represent a quantification of the number of pixels in a band, a measurement that is proportional to band intensity.

## RESULTS

### *Inheritance of Cortical ER Tubules in* S. cerevisiae

The inheritance of cortical ER was studied in live cells by using a previously characterized ER marker (Hmg1p-GFP; Hampton *et al.*, 1996; Cronin *et al.*, 2000) in which the $NH_2$-terminal transmembrane domain (1–702 amino acids) of the ER resident protein HMG-CoA reductase isozyme 1 (Hmg1p) was fused to the GFP and expressed from the strong constitutive TDH3 promoter. Although the overexpression of full-length Hmg1p causes the formation of nuclear-associated stacked membrane pairs (Wright *et al.*, 1988; Koning *et al.*, 1996), the Hmg1p-GFP used in this study does not contain the COOH terminus that is required for the formation of these membrane proliferations (Profant *et al.*, 1999). Both cortical and perinuclear ER, as well as cytoplasmic tubules, were readily detected in cells expressing this fusion protein (Figures 1A and 2A). We also observed a network of interconnected cortical ER tubules in focal planes close to the plasma membrane (our unpublished data), which has recently been described for other ER marker proteins (Prinz *et al.*, 2000).

When the distribution of Hmg1p-GFP-labeled ER was followed at all stages of the cell cycle in an asynchronous population of cells, <10% of the newly formed buds, with a volume smaller than 4% of the mother cell, contained detectable cortical ER tubules. Cortical ER tubules were seen in >90% of the daughter cells that grew slightly larger. Interestingly, cytoplasmic ER tubules oriented along the mother-bud axis were detected at the base of the bud or through the neck in cells containing newly formed buds that have no cortical ER (Figure 1A, top). These tubules were also observed in cells at later stages of the cell cycle (Figure 1A,

bottom) and in both haploid and diploid cells. As discussed later, electron microscopy also revealed that cytoplasmic ER tubules are transported into buds before ER tubules are observed at the periphery. In addition, no fragmentation or vesicularization of the ER was observed during mitosis.

Although microtubules do not play a role in the maintenance of ER structure in *S. cerevisiae* (Prinz *et al.*, 2000), they are essential for the migration of the nucleus and perinuclear ER into the mother-bud neck (Huffaker *et al.*, 1988; Jacobs *et al.*, 1988). To address the requirement of microtubules in the inheritance of cortical ER, we treated yeast cells with the microtubule-disrupting agent nocodazole. After 3 h, large budded mother cells that contained a single unelongated nucleus were mostly observed (Figure 1B). The daughter cells did not contain nuclei, however, they did contain cortical ER (Figure 1B). Thus, although it has been proposed that the perinuclear ER may be connected to the cortical ER network (Preuss *et al.*, 1991; Koning *et al.*, 1996), our results suggest that differential mechanisms may be involved in delivering these two different types of ER into the daughter cell.

### *Isolation of Tn3 Mutants*

Because the segregation of ER appears to be a highly ordered process, cortical ER inheritance is likely to be regulated by cellular proteins and cofactors. To identify the proteins involved in this event, we mutagenized cells expressing Hmg1p-GFP by randomly integrating a Tn3-based transposon into the genome as described previously (Burns *et al.*, 1994). From a collection of 3331 transformants, 17 mutants reproducibly displayed a delay in the delivery of ER into daughter cells. The overall structure of the ER in the mother cell of these mutants was the same as wild type. Below we report the characterization of one of these mutants, referred to as mutant 4.

When the phenotype of mutant 4 was compared with wild type, we observed many more small budded cells (>80% in the mutant verses <10% in wild type) that failed to acquire cortical and cytoplasmic ER tubules into the daughter cell (compare Figure 2B with A). More than 100 small buds with a volume between 4 and 13% of the mother were counted for this analysis. In larger buds that did not contain a nucleus, 100% of the wild-type, but only ~50% of the mutant cells, had acquired peripheral and cytoplasmic ER. A pronounced reduction in cytoplasmic ER components was even observed in some mutant buds that contained perinuclear ER (Figure 2B). The peripheral ER network was normal in most mutant buds before cytokinesis (our unpublished data) and the inheritance of nuclear-associated ER components also appeared to be unaffected.

To investigate whether the ER inherited late in the cell cycle in mutant 4 is cortical or perinuclear ER, cells were treated with nocodazole. After a 3-h incubation, the cells were arrested as large buds with a single unelongated nucleus in the mother cell. No notable decrease in cortical ER tubules in the large buds of nocodazole-treated mutant cells were detected compared with wild type (Figure 1B). Thus, we can conclude that in mutant 4 there is a delay in the segregation of cortical but not perinuclear ER.

The defects described above might reflect the mislocalization of Hmg1p-GFP or a delayed transmission of Hmg1p-GFP-labeled ER subcomponents. To test these possibilities, the distribution of ER in mutant 4 was examined by indirect immunofluorescence with the use of antibodies directed against Kar2p, a resident ER lumenal protein (Rose *et al.*, 1989), and Sec61p, an ER transmembrane protein (Wilkinson *et al.*, 1996). With this analysis, we confirmed the defect in cortical ER inheritance in mutant 4 with the use of two other marker proteins. As shown in Figure 3, A and B, both markers displayed a defect in cortical ER inheritance, demonstrating that the effects we observed were not specific to Hmg1p-GFP.

### *Molecular Cloning*

To determine whether the transposon inserted at a single locus, mutant 4 was crossed to wild type and the diploid cells were sporulated and dissected. The *LEU2* gene, that marks the transposon insertion, segregated 2:2 in the 34 tetrads examined. Twelve tetrads were also analyzed for defects in cortical ER inheritance. In all cases, the defect cosegregated with the *LEU2* gene. Cortical ER inheritance in diploid cells heterozygous for the transposon insertion was unaffected, indicating that the phenotype is recessive.

The location of the transposon in mutant 4 was mapped by a PCR-mediated method with the use of a pair of inverse primers that correspond to the transposon sequences (Adams *et al.*, 1997). Genomic DNA templates from the mutant gave a single 350-bp PCR product that was absent from wild type. This result, together with the tetrad analysis, indicated that mutant 4 contains a single transposon insertion. Analysis of the sequences adjacent to the transposon revealed that the insertion resides in the *AUX1/SWA2* gene, the product of which has recently been reported to be involved in clathrin function (Gall *et al.*, 2000; Pishvaee *et al.*, 2000). As a consequence of the insertion, 161 amino acids were truncated from the COOH terminus of Aux1p/Swa2p and 11 missense amino acids were added to the mutated protein (Figure 4A).

To verify we identified the correct gene, we constructed a mutant that lacks the genomic copy of *AUX1/SWA2* (*aux1/swa2*Δ). *aux1/swa2*Δ and *aux1/swa2::Tn3* (mutant 4) displayed similar defects in the transmission of cortical ER into buds (Figure 2C). The viability of *aux1/swa2*Δ haploid cells indicated that *AUX1/SWA2* is not essential for the vegetative growth of yeast cells. However, we reproducibly noticed that the growth of the *aux1/swa2::Tn3* and *aux1/swa2*Δ mutants was impaired at 25°C. These mutants grew well at 34 (Figure 3C), 30, and 37°C (data not shown), but were sick at 25°C and cold-sensitive for growth at 15°C (Figure 3C). The defect in cortical ER inheritance, however, was observed at all temperatures.

### *Sequence Analysis of the AUX1/SWA2 Gene*

As previously reported (Gall *et al.*, 2000; Pishvaee *et al.*, 2000), the *AUX1/SWA2* open reading frame encodes a protein of 668 amino acids. Analysis of the amino acid composition revealed that Aux1p/Swa2p is considerably rich in serine residues (12%). A BLAST database search with Aux1p/Swa2p identified one related open reading frame of unknown function in *S. pombe* (E value = $5.7 \times 10^{-21}$, accession no. CAB11512). The BLAST search also revealed the presence of a possible J-domain at the extreme COOH terminus as well as three potential tetratricopeptide repeat

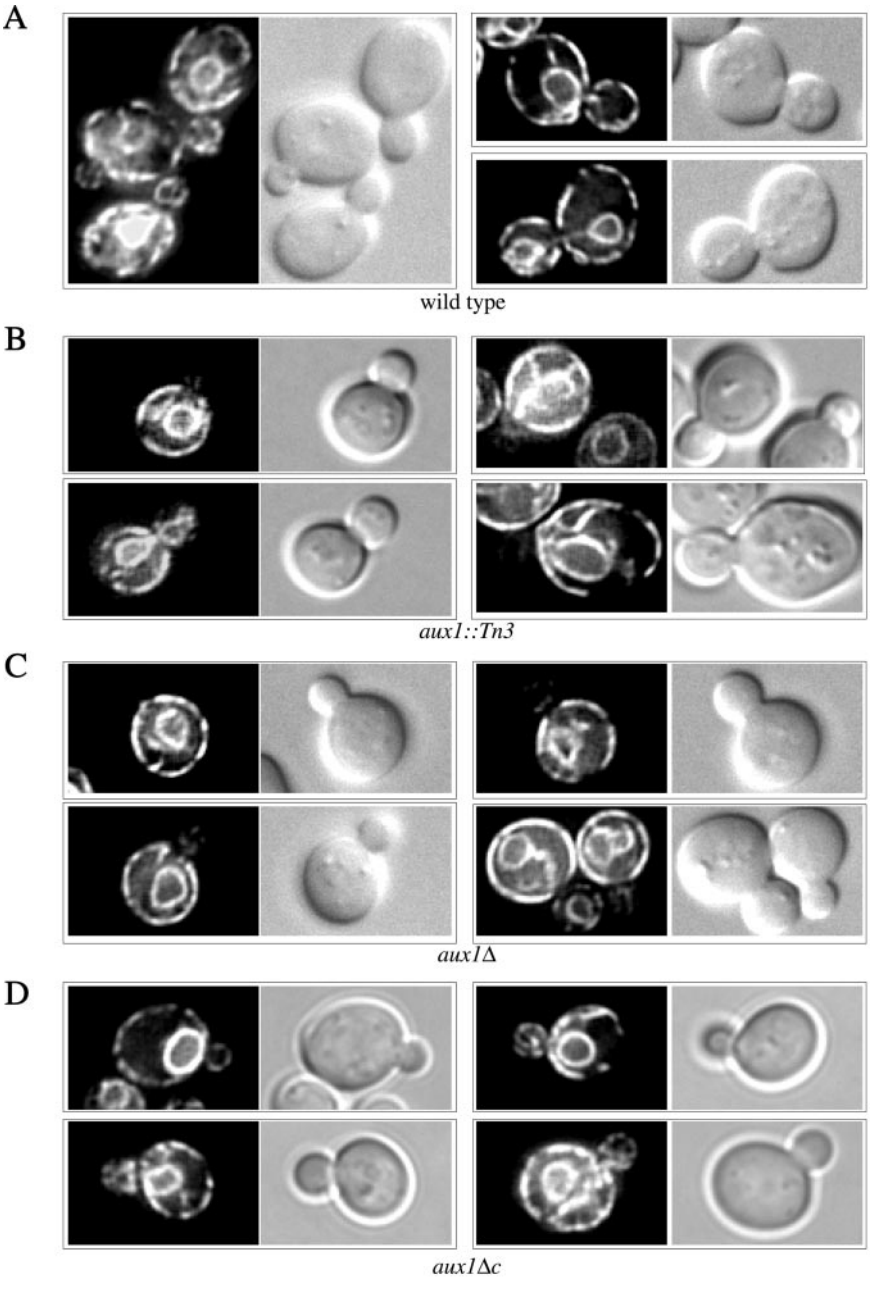


**Figure 2.** *aux1/swa2::Tn3* and *aux1/swa2*Δ, but not *aux1/swa2*Δ*c*, exhibit defects in cortical ER inheritance. Fluorescence microscopy and differential contrast images of wild type (A), *aux1/swa2::Tn3* (B), *aux1/swa2*Δ (C), and *aux1/swa2*Δ*c* (D) grown in YPD at 25°C.

(TPR) motifs in the central portion of Aux1p/Swa2p (amino acid 374–500, hereafter referred to as the Aux1p/Swa2p TPR domain; Figure 4B), The J-domain is a motif of ~70 amino acids that is conserved in Hsp40 family members and other Hsp70-binding cochaperones (Kelley, 1998).

The Aux1p/Swa2p J-domain has extensive sequence similarity to a subfamily of J-domains that are highly related to the J-domain of auxilin, a cochaperone involved in the uncoating of clathrin-coated vesicles (Holstein *et al.*, 1996). This domain of Aux1p/Swa2p stimulates Hsc70 to disassemble clathrin-coated vesicles in vitro. Furthermore, deletion of the J-domain of Aux1p/Swa2p results in the accumulation of clathrin-coated vesicles (Pishvaee *et al.*, 2000). The J-domain, combined with the $NH_2$-terminal clathrin binding domain (1–287 amino acids; Gall *et al.*, 2000) of Aux1p/Swa2p, may function as an auxilin-related cochaperone in the uncoating of clathrin-coated vesicles.

TPR motifs are degenerate 34 amino acid modules with a predicted helix-turn-helix conformation. Arrays of three or more tandem TPR motifs are frequently packed into a series of antiparallel super-helical structures to form TPR domains that mediate protein–protein interactions (Lamb *et al.* 1995; Das *et al.*, 1998; Scheufler *et al.*, 2000). TPR domains have been identified in a wide variety of proteins of diverse biological function. The TPR domain in Aux1p/Swa2p is not required to stimulate the ATPase activity of Hsp70 in vitro

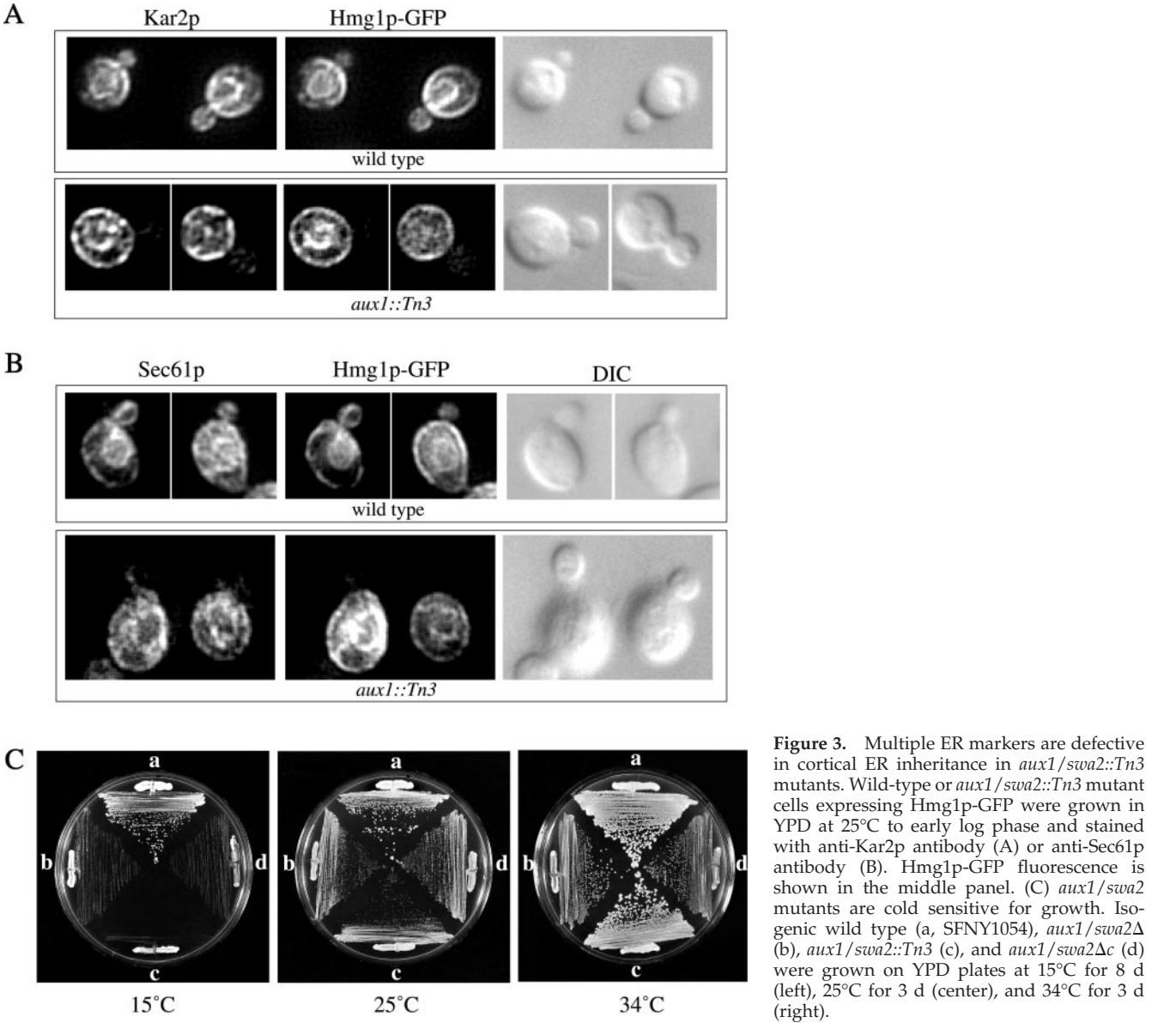


**Figure 3.** Multiple ER markers are defective in cortical ER inheritance in *aux1/swa2::Tn3* mutants. Wild-type or *aux1/swa2::Tn3* mutant cells expressing Hmg1p-GFP were grown in YPD at 25°C to early log phase and stained with anti-Kar2p antibody (A) or anti-Sec61p antibody (B). Hmg1p-GFP fluorescence is shown in the middle panel. (C) *aux1/swa2* mutants are cold sensitive for growth. Isogenic wild type (a, SFNY1054), *aux1/swa2*Δ (b), *aux1/swa2::Tn3* (c), and *aux1/swa2*Δ*c* (d) were grown on YPD plates at 15°C for 8 d (left), 25°C for 3 d (center), and 34°C for 3 d (right).

(Gall *et al.*, 2000). Interestingly, a point mutation in the Aux1p/Swa2p TPR domain displays synthetic lethal growth defects with *arf1*Δ (Gall *et al.*, 2000). One of the roles of Arf1p is to regulate the recruitment of clathrin to membranes (Stamnes and Rothman, 1993; Ooi *et al.*, 1998).

### *Inheritance of Other Organelles Appears to Be Unaffected in aux1/swa2Δ Mutant*

Like peripheral ER, the Golgi enters daughter cells at an early stage of bud growth (Preuss *et al.*, 1992). It has been suggested that early Golgi is derived from the ER and as a consequence is adjacent to transitional ER. The delocalized distribution of vesicle budding sites throughout the ER in *S. cerevisiae* would then result in the dispersed distribution of Golgi in the cytoplasm (Rossanese *et al.*, 1999). To determine whether the inheritance of Golgi membranes requires Aux1p/Swa2p function, we compared the distribution of Och1p in *aux1/swa2*Δ and wild-type cells. Och1p is a carbohydrate-modifying enzyme that defines one of the earliest Golgi compartments in yeast (Nakayama *et al.*, 1992; Brigance *et al.*, 2000). The distribution of a HA-tagged version of Och1p (Och1p-HA) was followed by indirect fluorescence with the use of anti-HA monoclonal antibody. Because small budded cells containing just cortical ER or just Och1p-HA–labeled Golgi were never observed in wild type, we conclude that these organelles are acquired at essentially the same time. When buds of similar size were compared, the number of Och1p-HA–labeled structures in mutant buds that lacked detectable ER staining was comparable to wild type (Figure 5A). Thus, the inheritance of *cis*-Golgi appears to be unaffected in *aux1/swa2*Δ.

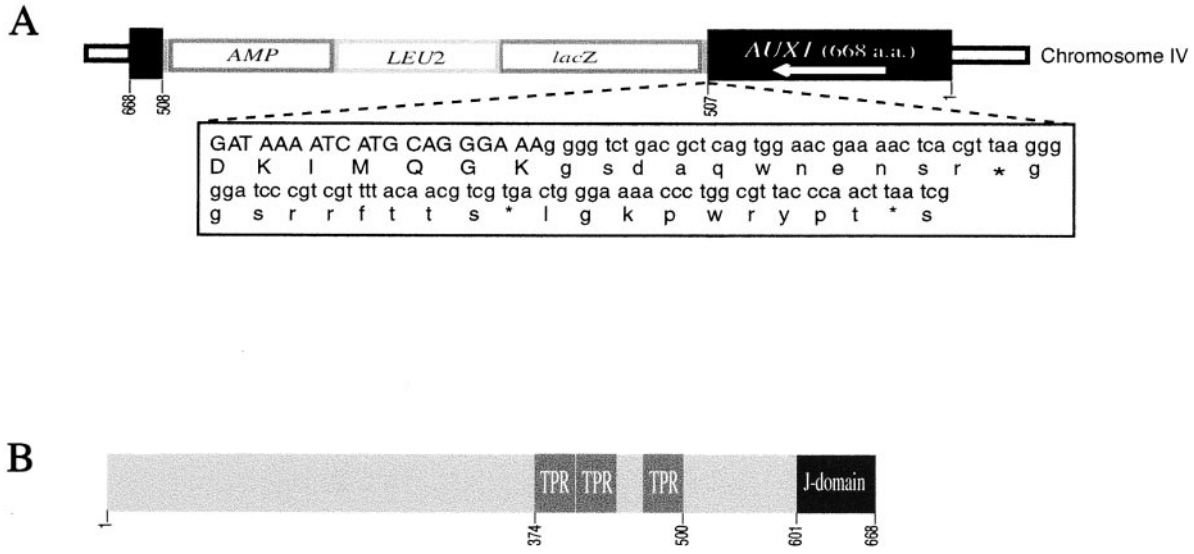


**Figure 4.** Chromosomal site of the *AUX1/SWA2* gene and predicted structural features of the *AUX1/SWA2* gene product. (A) Transposon insertion in *aux1/swa2::Tn3* maps in the *AUX1/SWA2* gene on chromosome IV. A single copy of the Tn3 derivative, which carries the 38-bp terminal Tn3 repeats (filled gray boxes), the yeast *LEU2* gene, and the bacterial AMP and *lacZ* genes is inserted 1521 bp downstream of the start codon. The DNA and corresponding amino acid sequences around the insertion are shown in a box. The *AUX1/SWA2* sequences are in uppercase and the Tn3 transposon sequences in lowercase. The asterisks indicate in-frame stop codons. (B) Aux1p/Swa2p protein contains a J-domain at the COOH terminus and three TPR motifs in the center.

The specific role of Aux1p/Swa2p in regulating cortical ER inheritance was examined further by comparing the distribution of mitochondria and vacuoles in *aux1/swa2*Δ and wild type. A close association between the ER and mitochondria has been described in both yeast and mammalian cells (Montisano *et al.* 1982; Perkins *et al.*, 1997; Prinz *et al.*, 2000). To study the distribution of mitochondria in the *aux1/swa2*Δ mutant, a plasmid (pYDY104) expressing a mitochondrial targeting sequence fused to RFP (Mozdy *et al.*, 2000) was transformed into wild-type and mutant cells. The migration of mitochondria into daughter cells was found to occur at an early stage of bud growth and was indistinguishable from wild type (Figure 5B).

To study vacuolar inheritance, vacuoles were labeled with the lipophilic vital dye FM4-64, which specifically stains the membrane of this organelle at steady state (Vida and Emr, 1995). In wild type, the appearance of vacuoles in buds occurred far behind the inheritance of peripheral ER (Figure 5C, left; Preuss *et al.*, 1991). Vacuoles were not observed in a high percentage of small budded cells (~50%) that had peripheral ER and buds containing vacuoles but not cortical ER were never observed. Strikingly, a large number of small vacuoles, similar to those seen in class B *vps* mutants (Raymond *et al.*, 1992), were dispersed throughout the cytoplasm of *aux1/swa2*Δ (Figure 5C, right). Based on these findings, we conclude that fragmented vacuoles are transported into *aux1/swa2*Δ buds that lack peripheral ER.

### *Deletion of J-domain of Aux1p/Swa2p Results in Vacuole Fragmentation and Membrane Accumulation*

The *aux1/swa2* mutants were compared with wild type at the ultrastructural level with the use of electron microscopy. To readily observe the plasma membrane and underlying ER tubules, intact cells were prepared for electron microscopy with the use of a method that slightly dilates the lumen of the ER (Mulholland *et al.*, 1994; Walch-Solimena *et al.*, 1997). In wild type, ER tubules followed secretory vesicles along the mother-bud axis into newly initiated buds (Figure 6A). As was observed by fluorescence microscopy, the inheritance of ER was dramatically delayed in *aux1/swa2::Tn3* and *aux1/swa2*Δ (Figure 6, B and C). Few or no ER tubules were seen in mutant buds that had mitochondria and vacuoles (Figure 6C; our unpublished data) and the fragmentation of vacuoles was also confirmed. To quantitate this phenotype, the number of vacuoles per cell surface area was counted. A significant increase in fragmented vacuoles was observed in *aux1/swa2*Δ compared with wild type (Figure 6E). This increase was less pronounced in *aux1/swa2::Tn3*. However, when the vacuoles were stained with FM4-64, the extent of vacuole fragmentation was the same in *aux1/swa2::Tn3* and *aux1/swa2*Δ (our unpublished data). Consistent with this finding, a filter overlay assay revealed that both *aux1/swa2*Δ and *aux1/swa2::Tn3* missort the soluble vacuolar protease carboxypeptidase Y (CPY) (our unpublished data).

Interestingly, electron microscopy revealed the accumulation of vesicles (see quantitation in Figure 6E) and aberrant membrane structures in both *aux1/swa2::Tn3* and *aux1/swa2*Δ. Clusters of 50–100-nm vesicles were found in the bud, mother, and neck (Figure 6, B and C). In addition, cup-shaped organelles were also found. These membranes resembled the aberrant Golgi-like structures, called Berkeley bodies, that have been observed in mutants that block protein transport through the Golgi apparatus (Novick *et al.*, 1980). Because the loss of Aux1p/Swa2p function did not affect the kinetics of invertase secretion (our unpublished data), it is unlikely that the accumulation of membranes is a consequence of blocking protein transport on the exocytic pathway.

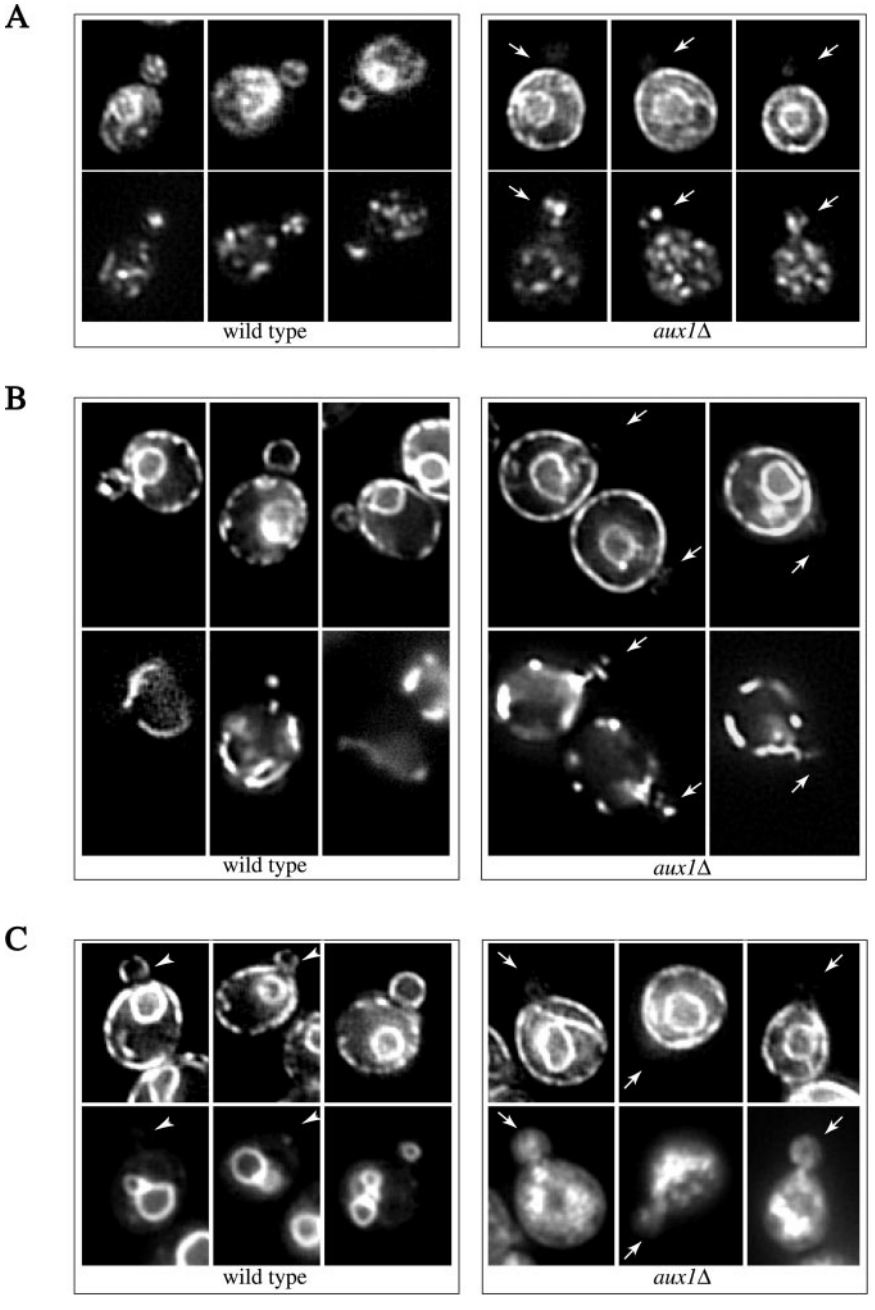


**Figure 5.** Other organelles are inherited in the *aux1/swa2*Δ mutant. (A) To visualize *cis*-Golgi, a plasmid expressing HA-tagged Och1p was transformed into wild type and *aux1/swa2*Δ. Cells were grown in minimal medium with the appropriate amino acids at 25°C and subjected to indirect immunofluorescence with the use of a monoclonal antibody directed against the HA epitope. (Top) Hmg1p-GFP fluorescence microscopy. (Bottom) Och1p-HA fluorescence microscopy. (B) To examine the distribution of mitochondria, pYDY104 was transformed into wild type and *aux1/swa2*Δ. Cells, expressing Hmg1p-GFP and a mitochondrial targeting sequence fused to RFP, were grown as described above and examined by fluorescence microscopy. The GFP- and RFP-tagged proteins are shown in the top and bottom panels, respectively. (C) Wild-type or *aux1/swa2*Δ cells, expressing Hmg1p-GFP were grown in YPD at 25°C and stained with 80 μM FM4-64 to visualize vacuoles. (Top) Hmg1p-GFP fluorescence microscopy. (Bottom) FM4-64 fluorescence microscopy. Arrows point to *aux1/swa2*Δ buds that contain little or no detectable cortical ER and arrowheads in C indicate small wild-type buds that only acquired cortical ER but not vacuoles.

The finding that the growth defect in the *aux1/swa2::Tn3* and *aux1/swa2*Δ mutants does not correlate with a defect in cortical ER inheritance suggested that Aux1p/Swa2p may be a bifunctional protein. For example, the COOH-terminal J-domain may be required for clathrin-uncoating activity, whereas the $NH_2$ terminus of Aux1p/Swa2p may be needed for cortical ER inheritance. To directly address this possibility, we constructed a mutant (*aux1/swa2*Δc) that truncates the COOH terminus of Aux1p/Swa2p, deleting the entire J-domain. Although *aux1/swa2*Δ*c* was cold sensitive for growth (Figure 3C), it was not defective in peripheral ER inheritance (Figure 2D). Thin section electron microscopy revealed that, like the *aux1/swa2::Tn3* and *aux1/swa2*Δ mutants, vacuoles were fragmented in *aux1/swa2*Δc (Figure 6, D and quantitation in E). The *aux1/swa2*Δ*c* mutant also accumulated vesicles (Figure 6, D and quantitation in E) and secreted CPY (our unpublished data). These findings support the hypothesis that Aux1p/Swa2p is a bifunctional protein.

### *Cortical ER Inheritance Is Not Affected in chc1 and arf1 Mutants*

To address whether the delay in cortical ER inheritance in *aux1/swa2*Δ is an indirect consequence of disrupting clathrin-mediated membrane transport, we examined the inher-

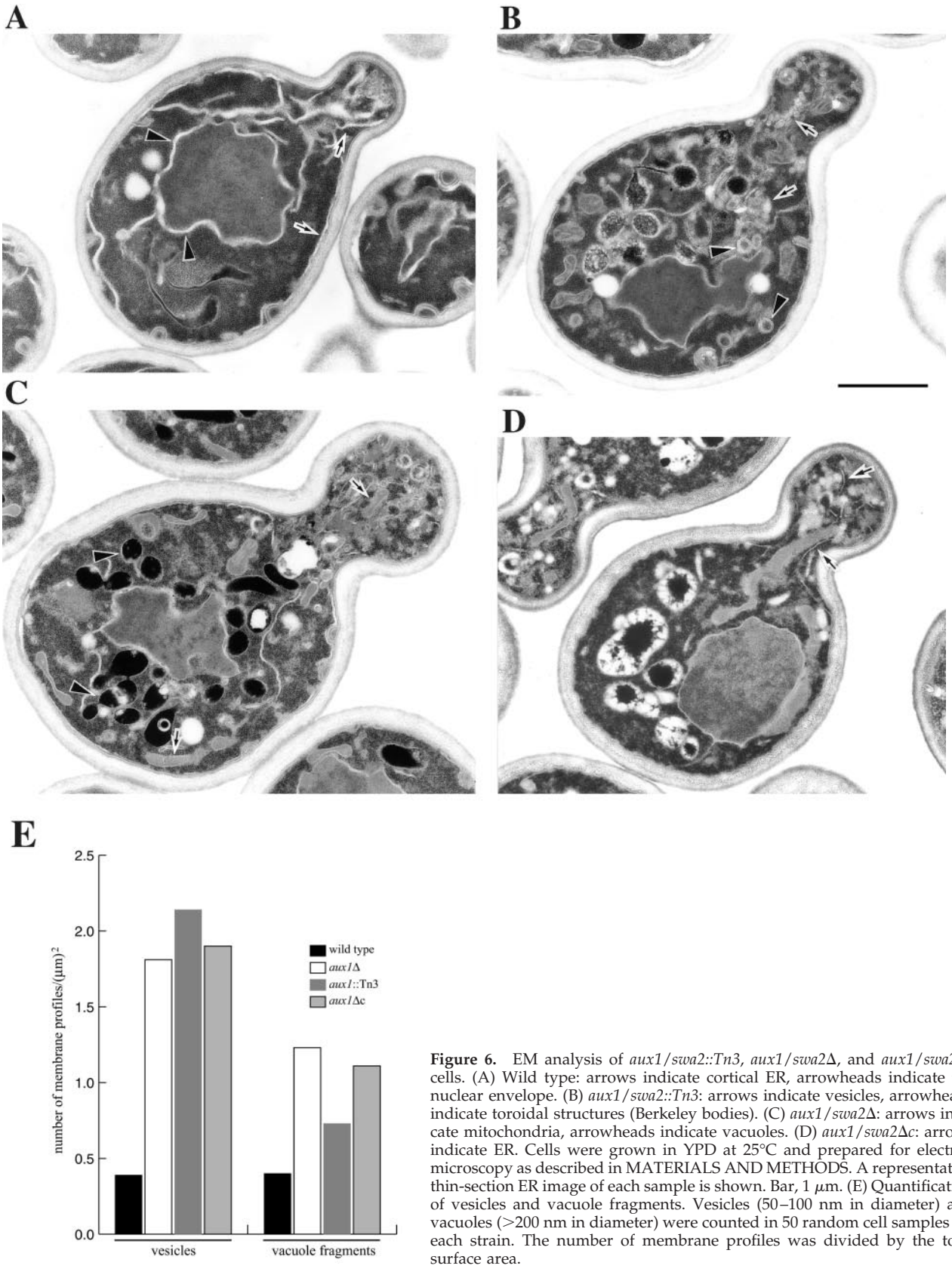


**Figure 6.** EM analysis of *aux1/swa2::Tn3*, *aux1/swa2*Δ, and *aux1/swa2*Δ*c* cells. (A) Wild type: arrows indicate cortical ER, arrowheads indicate the nuclear envelope. (B) *aux1/swa2::Tn3*: arrows indicate vesicles, arrowheads indicate toroidal structures (Berkeley bodies). (C) *aux1/swa2*Δ: arrows indicate mitochondria, arrowheads indicate vacuoles. (D) *aux1/swa2*Δ*c*: arrows indicate ER. Cells were grown in YPD at 25°C and prepared for electron microscopy as described in MATERIALS AND METHODS. A representative thin-section ER image of each sample is shown. Bar, 1 μm. (E) Quantification of vesicles and vacuole fragments. Vesicles (50–100 nm in diameter) and vacuoles (>200 nm in diameter) were counted in 50 random cell samples for each strain. The number of membrane profiles was divided by the total surface area.

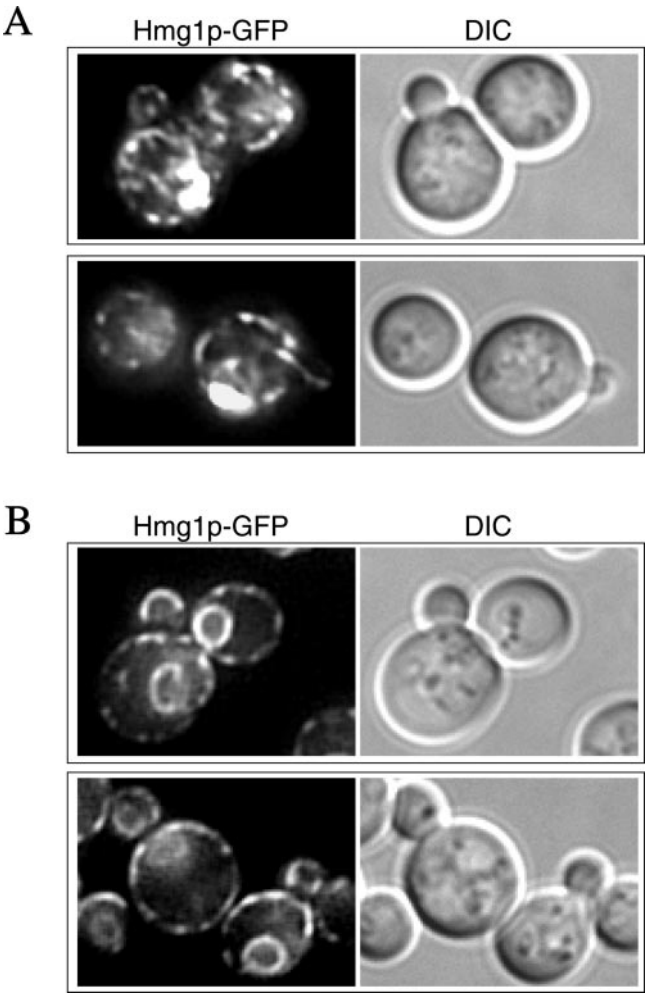


**Figure 7.** Cortical ER inheritance is normal in *chc1* and *arf1*Δ mutants. (A) Staining pattern of Hmg1p-GFP in *chc1-521*. Mutant cells were grown to early log phase at 25°C, shifted to 37°C for 3 h, and treated with 10 mM $NaN_3$. (B) Distribution of Hmg1p-GFP in *arf1*Δ grown at 25°C to early log phase. Representative cells with small buds are shown in B and the top of A. A cell with a newly formed bud containing an ER tubule through the neck is shown in the bottom panel of A.

itance of ER in *chc1-521*, a temperature-sensitive mutant defective in the clathrin heavy chain gene. After 3 h at the nonpermissive temperature (37°C), the majority of mutant cells showed brightly fluorescing spots or bundles in the cytoplasm (Figure 7A). These structures were not observed at the permissive temperature (25°C) and became obvious within 30 min at 37°C. Such structures were not observed in wild type. Although the cause of these brightly staining spots is unclear, the structure of the ER at the cell periphery and around the nucleus was the same as wild type. Furthermore, even after a 3-h shift to 37°C, the *chc1-521* mutant did not show a delay in the inheritance of cortical ER tubules (Figure 7A). More than 100 small buds with a volume between 4 and 13%of the mother cell were counted and 91% acquired cortical ER tubules. These results suggest that clathrin function is not required for regulating the inheritance of cortical ER tubules.

Because *ARF1* displays genetic interactions with both *CHC1* and *AUX1/SWA2* (Chen and Graham, 1998; Gall *et al.*, 2000), we determined whether Arf1p plays a role in mediating the segregation of cortical ER tubules. As shown in Figure 7B, the structure and inheritance of ER tubules in *arf1*Δ cells are essentially the same as wild type. More than 100 small buds were examined and 93% acquired cortical ER tubules. Thus, the loss of Arf1p function does not cause a delay in transmitting cortical ER tubules into daughter cells.

### *Aux1p/Swa2p Colocalizes with ER Membranes*

The subcellular localization of Aux1p/Swa2p was determined by fractionating lysates on a sucrose velocity gradient previously shown to resolve ER from Golgi membranes (Antebi and Fink, 1992; Barrowman *et al.*, 2000). Cell lysates were prepared from a wild-type strain and the distribution of this protein was monitored by Western blot analysis using an antibody directed against Aux1p/Swa2p. The immunoreactive band detected was not present in lysates prepared from an *aux1/swa2*Δ strain. In agreement with a previously published report (Pishvaee *et al.*, 2000), this band migrated with an apparent molecular weight of ~100 kDa. On this gradient, Aux1p/Swa2p cofractionated with the ER marker Bos1p (Figure 8A). We also compared the localization of Aux1p/Swa2p with that of Bet1p, a SNAP-25-related protein that is found on both ER and Golgi membranes (Barrowman *et al.*, 2000). Aux1p/Swa2p cofractionated with the ER peak of Bet1p, and not with the portion of Bet1p that is found on the Golgi. In addition, Aux1p/Swa2p did not colocalize with Pep12p, an endosomal marker (Becherer *et al.*, 1996), or clathrin (Figure 8A). Thus, these findings indicate that Aux1p/Swa2p is found on the ER and not on Golgi or endosomes.

To further characterize the intracellular localization of Aux1p/Swa2p, we tagged the genomic copy of *AUX1/SWA2* with GFP at its 3′ end. This fusion protein was functional because it did not affect the growth of wild-type cells or lead to a delay in the inheritance of cortical ER (our unpublished data). As shown in Figure 8B, weakly fluorescing dots were observed in cells expressing the Aux1p/Swa2p-GFP fusion protein. Interestingly, the majority of these dots were detected along the cell periphery where the cortical ER resides and not around the nucleus. Because subcellular fractionation studies have shown that Aux1p/Swa2p is on the ER (Figure 8A), these dots may represent a substructure of the cortical ER. However, we were unable to colocalize these structures with Hmg1p-GFP because the staining pattern of HA tagged Aux1p/Swa2p on membranes was perturbed by fixation.

## DISCUSSION

Here we have demonstrated that the disruption of *AUX1/SWA2* causes a delay in the transport of cortical ER elements into daughter cells. The loss of Aux1p/Swa2p function specifically affects the inheritance of cortical ER, but not the general morphology of the ER. The *aux1/swa2* mutation does not disrupt the segregation of the nucleus or nuclear-associated ER elements. Other intracellular organelles, such as *cis*-Golgi, mitochondria, and vacuoles, are readily detected

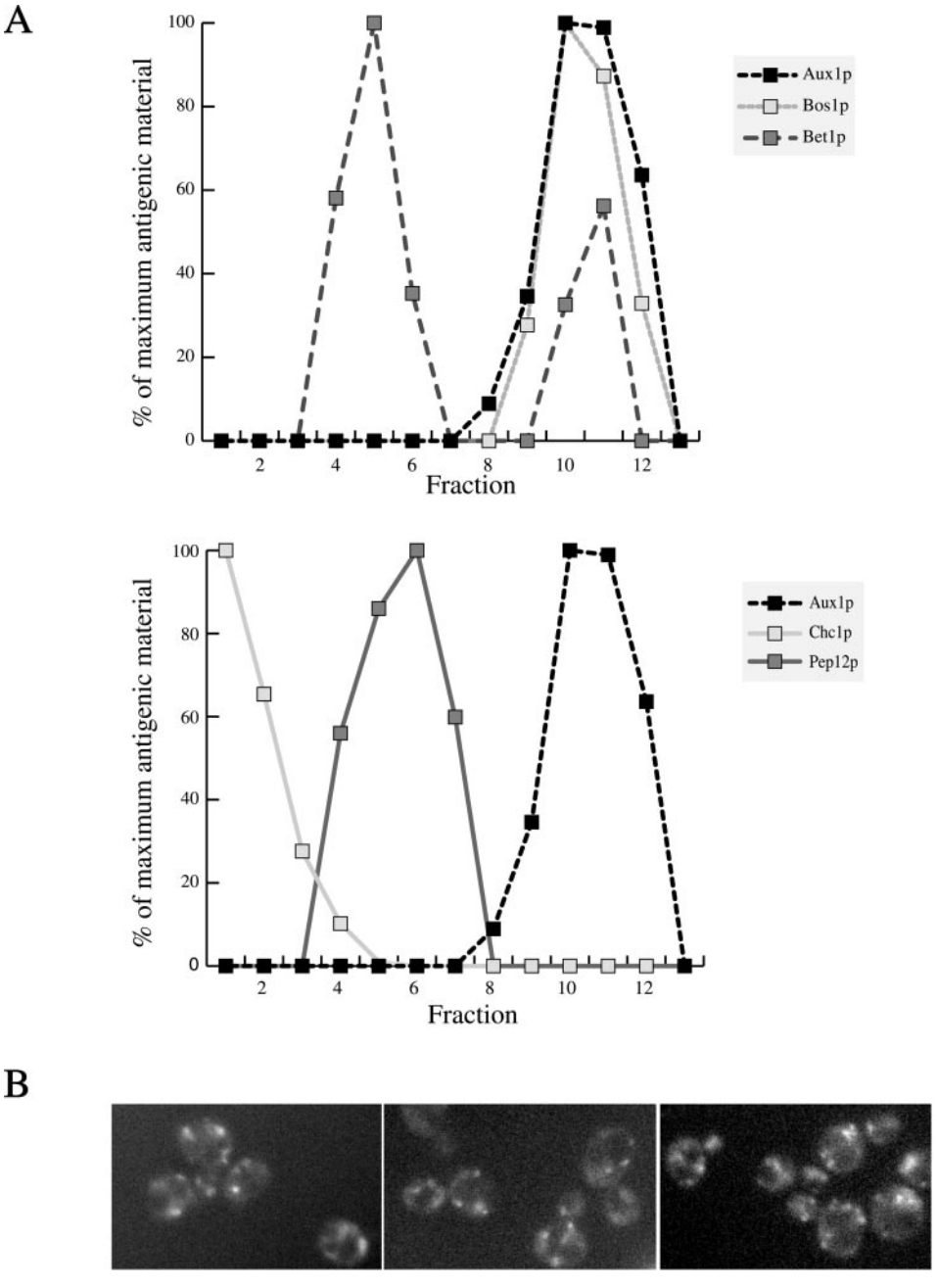


**Figure 8.** (A) Aux1p/Swa2p Colocalizes with ER membranes. Aux1p/Swa2p (■) cofractionates with Bos1p (□), an ER marker, and with the ER peak of Bet1p (▨) on a sucrose velocity gradient. In contrast, Pep12p (▨), an endosomal marker, and Chc1p (□), do not cofractionate with Aux1p/Swa2p. (B) Aux1p/Swa2p-GFP displays a punctate fluorescing pattern along the cell periphery. Cells expressing Aux1p/Swa2p-GFP were grown at 25°C in minimal medium with the appropriate amino acids to early log phase. Three representative fields are shown.

in *aux1/swa2* daughter cells that have no or substantially reduced amounts of cortical ER. *AUX1/SWA2* has recently been reported to encode an auxilin-related cochaperone involved in the uncoating of clathrin-coated vesicles (Gall *et al.*, 2000; Pishvaee *et al.*, 2000). However, loss of function of either Chc1p or Arf1p, two components of clathrin-coated vesicles that show physical or genetic interactions with Aux1p/Swa2p (Gall *et al.*, 2000; Pishvaee *et al.*, 2000), does not perturb cortical ER inheritance. Aux1p/Swa2p cofractionates with ER markers on a sucrose velocity gradient. Together, our findings indicate that Aux1p/Swa2p is a bifunctional protein involved in the inheritance of cortical ER during the yeast cell cycle and clathrin-mediated membrane traffic.

Given that the yeast ER retains its integrity during mitotic division (Preuss *et al.*, 1991), it has been proposed that the inheritance of this organelle is an active process (Warren and Wickner, 1996). Results presented here provide further support for this idea. In nocodazole-treated cells, daughter cells appear to acquire the same amount of cortical ER as the mother. This finding, together with the observation that cortical ER is inherited well before the nucleus in wild type, indicates that the migration of perinuclear ER into buds is not required for

proper partitioning of cortical ER. This in turn implies that cortical ER does not originate from the nuclear envelope in the bud. Both fluorescence and electron microscopy reveal that newly initiated buds lack ER tubules closely opposed to the plasma membrane. The first ER elements detectable in the bud are cytoplasmic ER tubules frequently oriented along the mother-bud axis. These observations imply that cortical ER is not passively pulled into the daughter cell by the expanding plasma membrane. Instead, it is likely to be transported into the bud in the form of cytoplasmic tubules that are then propagated to the cortical region. Furthermore, the isolation of the *aux1/swa2* mutant clearly indicates that cortical ER inheritance is mediated by cellular proteins.

By fluorescence and electron microscopy, we have shown that the structure and amount of ER that is adjacent to the plasma membrane in the mother cells of *aux1/swa2* mutants appear to be comparable to wild type. This property distinguishes *aux1/swa2* mutants from two classes of ER inheritance mutants recently reported (Prinz *et al.*, 2000). One class of mutants disrupts membrane transport between the ER and Golgi, and the ER segregation defect is thought to be a result of the mislocalization of resident ER proteins. The second class has defects in components of the signal recognition particle or the signal recognition particle receptor that is required for ribosome–ER association. The abnormal ER distribution has been proposed to be caused by the failure of ribosomes to bind to the ER (Prinz *et al.*, 2000). The *aux1/swa2* mutants do not exhibit several of the phenotypes that are observed in these two classes of mutants. These phenotypes include a substantial decrease of cortical ER tubules in the periphery of mother cells, accumulation of abnormal ER structures throughout the cytoplasm, and fragmentation of mitochondria. Beyond the ER structure, the function of the ER in protein transport also seems to be normal in the *aux1/swa2* mutants. The kinetics of invertase secretion (our unpublished observation), pro-α-factor secretion (Gall *et al.*, 2000), and transport of alkaline phosphatase to vacuoles (Pishvaee *et al.*, 2000) in *aux1/swa2* mutants is comparable to that in wild-type cells. Therefore, the delayed ER inheritance phenotype in *aux1/swa2* is unlikely to be a consequence of a general disruption of ER structure or function.

The cortical ER of yeast has been proposed to have physical and/or functional connections with the nucleus and mitochondria. It forms a continuous network connected by a few cytoplasmic tubules to the perinuclear ER (Preuss *et al.*, 1991; Koning *et al.*, 1996). Close contacts between subfractions of the cortical ER and mitochondria (Gaigg *et al.*, 1995; Prinz *et al.*, 2000) have been thought to facilitate interorganelle transport of phospholipid (Achleitner *et al.*, 1999). Mutations disrupting cortical ER structure cause the mitochondria to fragment, and it has been suggested that the structure of the cortical ER determines that of the mitochondria (Prinz *et al.*, 2000). Despite these possible connections, our findings indicate that partitioning of the nuclear envelope and mitochondria is essentially normal in *aux1/swa2* mutants and suggests that segregation of these two organelles is independent of cortical ER inheritance. Distinct molecular components may be involved in mediating ER inheritance, structure, and function.

A correlation between the distribution of transitional ER subdomains and that of the *cis*-Golgi in yeast has led to the proposal that the Golgi is formed by the fusion of ER-derived vesicles (Rossanese *et al.*, 1999). The normal distribution of Golgi in *aux1/swa2* mutant buds that contain few or no ER tubules suggests that Golgi inheritance is an active process that is independent of ER inheritance. Based on immunoelectron studies showing Golgi structures clustered at the base of newly initiated buds and transported through the neck of budded cells, active transport of the Golgi apparatus was proposed earlier (Preuss *et al.*, 1992).

Consistent with results from two other groups (Gall *et al.*, 2000; Pishvaee *et al.*, 2000), we found that in addition to cortical ER inheritance, Aux1p/Swa2p is involved in other cellular processes. The *aux1/swa2* mutants displayed severe growth defects at temperatures below 25°C, whereas the ER inheritance phenotype was seen at all temperatures. The loss of Aux1p/Swa2p function causes vesicle accumulation, vacuole fragmentation, and CPY missorting, which may reflect its role in the disassembly of clathrin-coated vesicles. Because *aux1/swa2* mutants accumulate vesicles that are concentrated in the bud, one might speculate that the ER inheritance defect in *aux1/swa2* mutants is an indirect result of steric interference by these vesicles. However, in agreement with a previous report (Prinz *et al.*, 2000), we find that ER inheritance is not affected in post-Golgi blocked *sec* mutants, which accumulate more vesicles in the bud than *aux1/swa2* (our unpublished data).

Our results provide several lines of evidence suggesting that the delayed inheritance of cortical ER in *aux1/swa2* mutants is not a consequence of interrupted clathrin-regulated cellular processes. First, the inheritance of cortical ER was normal in an *aux1/swa2*Δ*c* mutant lacking the J-domain required for membrane trafficking. This result clearly indicates that the role of Aux1p/Swa2p in regulating cortical ER inheritance can be uncoupled from its role in clathrin function. Second, the inheritance of cortical ER was unaffected after a 3-h shift to 37°C in the *chc1-521* mutant, which is defective in trimerization and association with the light chain of clathrin (Pishvaee *et al.*, 1997). The *chc1-521* mutant displays temperature-sensitive defects in most, if not all, clathrin-dependent cellular processes, including growth, endocytosis, retention of post-Golgi membrane proteins and CPY sorting (Seeger and Payne, 1992a,b; Tan *et al.*, 1993). It has been shown that the *chc1-521* mutant regains the ability to sort CPY after a 3-h shift to 37°C. However, because ER inheritance is also normal in the *chc1-521* mutant after a 30-min shift to 37°C (our unpublished observation), we can exclude the possibility that mutant cells use a clathrin-independent adaptation pathway to regulate cortical ER inheritance. Third, complete disruption of the *ARF1* gene does not cause a defect in cortical ER inheritance. Taken together, these results indicate that blocking the formation of clathrin-coated vesicles does not perturb the transmission of cortical ER tubules into the bud.

Our finding of a physical association of Aux1p/Swa2p with the ER by subcellular fractionation studies supports a direct role for this protein on the ER. All Aux1p/Swa2p was found to reside on the ER by sucrose velocity gradient fractionation. However, we cannot exclude the possibilities that due to degradation or the sensitivity of our assay a portion of Aux1p/Swa2p was soluble or associated with another structure. Because fluorescence microscopy did not reveal Aux1p/Swa2p-GFP on nuclear-associated ER, this is the first example to our knowledge of a protein that specifically associates with cortical ER tubules. The observed punctate structures might represent subdomains of cortical ER tubules. The nature of these substructures and their functional significance in the inheritance of cortical ER are intriguing issues for future study.

Based on the results from this study, we propose that Aux1p/Swa2p is a protein involved in multiple cellular processes that include the inheritance of cortical ER and the uncoating of clathrin-coated vesicles. Future studies on the identification and characterization of Aux1p/Swa2p-associated proteins may shed light on the mechanisms by which these processes are mediated in cells.

## ACKNOWLEDGMENTS

We thank Randy Hampton for providing pRH475 before publication; Janet Shaw, John Pringle, Gerry Waters, David Botstein, and Gregory Payne for strains and plasmids; Mike Snyder for the Tn3-based transposon-mutagenized yeast genomic DNA library; and Mark Rose, Jeff Brodsky, and Gregory Payne for antibodies. We also thank Monica Andreoli, Elaine Downie, and Lora Cavallo for technical assistance, and Joyce Anquillare for help in the preparation of this manuscript. Yunrui Du is a postdoctoral associate of the Howard Hughes Medical Institute. This work was supported by a program project grant from the National Cancer Institute (to S.F.-N. and P.N.).

## REFERENCES

Achleitner, G., Gaigg, B., Krasser, A., Kainersdorfer, E., Kohlwein, S.D., Perktold, A., Zellnig, G., and Daum, G. (1999). Association between the endoplasmic reticulum and mitochondria of yeast facilitates interorganelle transport of phospholipids through membrane contact. Eur. J. Biochem. *264*, 545–553.

Adams, A., Gottschling, D.E., Kaiser, C.A., and Stearns, T. (1997). Methods in Yeast Genetics. Cold Spring Harbor, NY: Cold Spring Harbor Laboratory Press, 85–92.

Antebi, A., and Fink, G.R. (1992). The yeast Ca(2+)-ATPase homologue, PMR1, is required for normal Golgi function and localizes in a novel Golgi-like distribution. Mol. Biol. Cell *3*, 633–654.

Baba, M., and Osumi, M. (1987). Transmission and scanning electron microscope examination of intracellular organelles in freeze-substituted *Kloeckera* and *Saccharomyces cerevisiae* yeast cells. J. Electron Microsc. Technol. *5*, 249–261.

Barrowman, J., Sacher, M., and Ferro-Novick, S. (2000). TRAPP stably associates with the Golgi and is required for vesicle docking. EMBO J. *19*, 862–869.

Becherer, K.A., Rieder, S.E., Emr, S.D., and Jones, E.W. (1996). Novel syntaxin homologue, Pep12p, required for the sorting of lumenal hydrolases to the lysosome-like vacuolein yeast. Mol. Biol. Cell *7*, 579–594.

Brigance, W.T., Barlowe, C., and Graham, T.R. (2000). Organization of the yeast Golgi complex into at least four functionally distinct compartments. Mol. Biol. Cell *11*, 171–182.

Burns, N., Grimwade, B., Ross-Macdonald, P.B., Choi, E.Y., Finberg, K., Roeder, G.S., and Snyder, M. (1994). Large-scale analysis of gene expression, protein localization, and gene disruption in *Saccharomyces cerevisiae*. Genes Dev. *8*, 1087–1105.

Chen, C.Y., and Graham, T.R. (1998). An *arf1*Δ synthetic lethal screen identifies a new clathrin heavy chain conditional allele that perturbs vacuolar protein transport in *Saccharomyces cerevisiae*. Genetics *150*, 577–589.

Cronin, S.R., Khoury, A., Ferry, D.K., and Hampton, R.Y. (2000). Regulation of HMG-CoA reductase degradation requires the P-type ATPase Cod1p/Spf1p. J. Cell Biol. *148*, 915–924.

Das, A.K., Cohen, P.W., and Barford, D. (1998). The structure of the tetratricopeptide repeats of protein phosphatase 5: implications for TPR-mediated protein-protein interactions. EMBO J. *17*, 1192–1199.

Ellenberg, J., Siggia, E.D., Moreira, J.E., Smith, C.L., Presley, J.F., Worman, H.J., and Lippincott-Schwartz, J. (1997). Nuclear membrane dynamics and reassembly in living cells: targeting of an inner nuclear membrane protein in interphase and mitosis. J. Cell Biol. *138*, 1193–1206.

Gaigg, B., Simbeni, R., Hrastnik, C., Paltauf, F., and Daum, G. (1995). Characterization of a microsomal subfraction associated with mitochondria of the yeast, *Saccharomyces cerevisiae*. Involvement in synthesis and import of phospholipids into mitochondria. Biochim. Biophys. Acta *1234*, 214–220.

Gall, W.E., Higginbotham, M.A., Chen, C., Ingram, M.F., Cyr, D.M., and Graham, T.R. (2000). The auxilin-like phosphoprotein Swa2p is required for clathrin function in yeast. Curr. Biol. *10*, 1349–1358.

Hampton, R.Y., Koning, A., Wright, R., and Rine, J. (1996). *In vivo* examination of membrane protein localization and degradation with green fluorescent protein. Proc. Natl. Acad. Sci. USA *93*, 828–833.

Holstein, S.E., Ungewickell, H., and Ungewickell, E. (1996). Mechanism of clathrin basket dissociation: separate functions of protein domains of the DnaJ homologue auxilin. J. Cell Biol. *135*, 925–937.

Huffaker, T.C., Thomas, J.H., and Botstein, D. (1988). Diverse effects of beta-tubulin mutations on microtubule formation and function. J. Cell Biol. *106*, 1997–2010.

Ioshii, S.O., Yoshida, T., Imanaka-Yoshida, K., and Izutsu, K. (1995). Distribution of a $Ca2^{+}$ storing site in PtK2 cells during interphase and mitosis. An immunocytochemical study using an antibody against calreticulin. Eur. J. Cell Biol. *66*, 82–93.

Jacobs, C.W., Adams, A.E., Szaniszlo, P.J., and Pringle, J.R. (1988). Functions of microtubules in the *Saccharomyces cerevisiae* cell cycle. J. Cell Biol. *107*, 1409–1426.

Kelley, W.L. (1998). The J-domain family and the recruitment of chaperone power. Trends Biochem. Sci. *23*, 222–227.

Koning, A.J., Roberts, C.J., and Wright, R.L. (1996). Different subcellular localization of *Saccharomyces cerevisiae* HMG-CoA reductase isozymes at elevated levels corresponds to distinct endoplasmic reticulum membrane proliferations. Mol. Biol. Cell *7*, 769–789.

Lamb, J.R., Tugendreich, S., and Hieter, P. (1995). Tetratrico peptide repeat interactions: to TPR or not to TPR? Trends Biochem. Sci. *20*, 257–259.

Lee, C., and Chen, L.B. (1988). Dynamic behavior of endoplasmic reticulum in living cells. Cell. *54*, 37–46.

Longtine, M.S., McKenzie, A., Demarini, D.J., Shah, N.G., Wach, A., Brachat, A., Philippsen, P., and Pringle, J.R. (1998). Additional modules for versatile and economical PCR-based gene deletion and modification in *Saccharomyces cerevisiae*. Yeast. *14*, 953–961.

Marshall, I.C.B., and Wilson, K.L. (1997). Nuclear envelop assembly after mitosis. Trends Cell Biol. *7*, 69–74.

McConnell, S.J., Stewart, L.C., Talin, A., and Yaffe, M.P. (1990). Temperature-sensitive yeast mutants defective in mitochondrial inheritance. J. Cell Biol. *111*, 967–976.

Montisano, D.F., Cascarano, J., Pickett, C.B., and James, T.W. (1982). Association between mitochondria and rough endoplasmic reticulum in rat liver. Anat. Rec. *203*, 441–450.

Mozdy, A.D., McCaffery, J.M., and Shaw, J.M. (2000). Dnm1p GTPase-mediated mitochondrial fission is a multi-step process requiring the novel integral membrane component Fis1p. J. Cell Biol. *151*, 367–380.

Mulholland, J., Preuss, D., Moon, A., Wong, A., Drubin, D., and Botstein, D. (1994). Ultrastructure of the yeast actin cytoskeleton and its association with the plasma membrane. J. Cell Biol. *125*, 381–391.

Mumberg, D., Muller, R., and Funk, M. (1995). Yeast vectors for the controlled expression of heterologous proteins in different genetic backgrounds. Gene *156*, 119–122.

Nakayama, K., Nagasu, T., Shimma, Y., Kuromitsu, J., and Jigami, Y. (1992). *OCH1* encodes a novel membrane bound mannosyltransferase: outer chain elongation of asparagine-linked oligosaccharides. EMBO J. *11*, 2511–2519.

Novick, P., Field, C., and Schekman, R. (1980). Identification of 23 complementation groups required for post-translational events in the yeast secretory pathway. Cell *21*, 205–215.

Nunnari, J., and Walter, P. (1996). Regulation of organelle biogenesis. Cell. *84*, 389–394.

Ooi, C.E., Dell'Angelica, E.C., and Bonifacino, J.S. (1998). ADP-Ribosylation factor 1 (ARF1) regulates recruitment of the AP-3 adaptor complex to membranes. J. Cell Biol. *142*, 391–402.

Palade, G.E. (1956). The endoplasmic reticulum. J. Biophys. Biochem. Cytol. *2*, 85–98.

Perkins, G., Renken, C., Martone, M.E., Young, S.J., Ellisman, M., and Frey, T. (1997). Electron tomography of neuronal mitochondria: three-dimensional structure and organization of cristae and membrane contacts. J. Struct. Biol. *119*, 260–272.

Pishvaee, B., Costaguta, G., Yeung, B.G., Ryazantsev, S., Greener, T., Greene, L.E., Eisenberg, E., McCaffery, J.M., and Payne, G.S. (2000). A yeast DNA J protein required for uncoating of clathrin-coated vesicles *in vivo*. Nat. Cell Biol. *2*, 958–963.

Pishvaee, B., Munn, A., and Payne, G.S. (1997). A novel structural model for regulation of clathrin function. EMBO J. *16*, 2227–2239.

Preuss, D., Mulholland, J., Franzusoff, A., Segev, N., and Botstein, D. (1992). Characterization of the *Saccharomyces* Golgi complex through the cell cycle by immunoelectron microscopy. Mol. Biol. Cell *3*, 789–803.

Preuss, D., Mulholland, J., Kaiser, C.A., Orlean, P., Albright, C., Rose, M.D., Robbins, P.W., and Botstein, D. (1991). Structure of the yeast endoplasmic reticulum: localization of ER proteins. Yeast. *7*, 891–911.

Prinz, W.A., Grzyb, L., Veenhuis, M., Kahana, J.A., Silver, P.A., and Rapoport, T.A. (2000). Mutants affecting the structure of the cortical endoplasmic reticulum in *Saccharomyces cerevisiae*. J. Cell Biol. *150*, 461–474.

Profant, D.A., Roberts, C.J., Koning, A.J., and Wright, R.L. (1999). The role of the 3-hydroxy 3-methylglutaryl coenzyme A reductase cytosolic domain in karmellae biogenesis. Mol. Biol. Cell *10*, 3409–3423.

Raymond, C.K., Howald-Stevenson, I., Vater, C.A., and Stevens, T.H. (1992). Morphological classification of the yeast vacuolar protein sorting mutants: evidence for a prevacuolar compartment in class E vps mutants. Mol. Biol. Cell *3*, 1389–1402.

Rose, M.D., Misra, L.M., and Vogel, J.P. (1989). *KAR2*, a karyogamy gene, is the yeast homolog of the mammalian BiP/*GRP78* gene. Cell *57*, 1211–1221.

Rossanese, O.W., Soderholm, J., Bevis, B.J., Sears, I.B., O'Connor, J., Williamson, E.K., and Glick, B.S. (1999). Golgi structure correlates with transitional endoplasmic reticulum organization in *Pichia pastoris* and *Saccharomyces cerevisiae*. J. Cell Biol. *145*, 69–81.

Scheufler, C., Brinker, A., Bourenkov, G., Pegoraro, S., L. Moroder, L., Bartunik, H., Hartl, F.U., and Moarefi, I. (2000). Structure of TPR domain-peptide complexes: critical elements in the assembly of the Hsp70-Hsp90 multichaperone machine. Cell *101*, 199–210.

Seeger, M., and Payne, G.S. (1992a). A role for clathrin in the sorting of vacuolar proteins in the Golgi complex of yeast. EMBO J. *11*, 2811–2818.

Seeger, M., and Payne, G.S. (1992b). Selective and immediate effects of clathrin heavy chain mutations on Golgi membrane protein retention in *Saccharomyces cerevisiae*. J. Cell Biol. *118*, 531–540.

Stamnes, M.A., and Rothman, J.E. (1993). The binding of AP-1 clathrin adaptor particles to Golgi membranes requires ADP-ribosylation factor, a small GTP-binding protein. Cell *73*, 999–1005.

Tan, P.K., Davis, N.G., Sprague, G.F., and Payne, G.S. (1993). Clathrin facilitates the internalization of seven transmembrane segment receptors for mating pheromones in yeast. J. Cell Biol. *123*, 1707–1716.

Terasaki, M. (2000). Dynamics of the endoplasmic reticulum and Golgi apparatus during early sea urchin development. Mol. Biol. Cell *11*, 897–914.

Vida, T.A., and Emr, S.D. (1995). A new vital stain for visualizing vacuolar membrane dynamics and endocytosis in yeast. J. Cell Biol. *128*, 779–792.

Walch-Solimena, C., Collins, R.N., and Novick, P.J. (1997). Sec2p mediates nucleotide exchange on Sec4p and is involved in polarized delivery of post-Golgi vesicles. J. Cell Biol. *137*, 1495–1509.

Wang, Y.X., Zhao, H., Harding, T.M., Gomes, D., Mesquita, D.S., Woldringh, C.L., Klionsky, D.J., Munn, A.L., and Weisman, L.S. (1996). Multiple classes of yeast mutants are defective in vacuole partitioning yet target vacuole proteins correctly. Mol. Biol. Cell *7*, 1375–1389.

Warren, G., and Wickner, W. (1996). Organelle inheritance. Cell *84*, 395–400.

Waterman-Storer, C.M., Sanger, J.W., and Sanger, J.M. (1993). Dynamics of organelles in the mitotic spindles of living cells: membrane and microtubule interactions. Cell Motil. Cytoskeleton *26*, 19–39.

Weisman, L.S., Emr, S.D., and Wickner, W.T. (1990). Mutants of *Saccharomyces cerevisiae* that block intervacuole vesicular traffic and vacuole division and segregation. Proc. Natl. Acad. Sci. USA *87*, 1076–1080.

Wiese, C., and Wilson, K.L. (1993). Nuclear membrane dynamics. Curr. Opin. Cell Biol. *5*, 387–394.

Wilkinson, B.M., Critchley, A.J., and Stirling, C.J. (1996). Determination of the transmembrane topology of yeast Sec61p, an essential component of the endoplasmic reticulum translocation complex. J. Biol. Chem. *271*, 25590–25597.

Wilson, K.L. (2000). The nuclear envelop, muscular dystrophy, and gene expression. Trends Cell Biol. *10*, 125–129.

Wright, R., Basson, M., D'Ari, L., and Rine, R. (1988). Increased amounts of HMG-CoA reductase induce "karmellae": a proliferation of stacked membrane pairs surrounding the yeast nucleus. J. Cell Biol. *107*, 101–114.

Yaffe, M.P. (1999). The machinery of mitochondrial inheritance and behavior. Science *283*, 1493–1497.

Yang, L., Guan, T., and Gerace, L. (1997). Integral membrane proteins of the nuclear envelope are dispersed throughout the endoplasmic reticulum during mitosis. J. Cell Biol. *137*, 1199–1210.

Zeligs, J.D., and Wollman, S.H. (1979). Mitosis in rat thyroid epithelial cells *in vivo*. I. Ultrastructural changes in cytoplasmic organelles during the mitotic cycle. J. Ultrastruct. Res. *66*, 53–77.